Geomechanics and Engineering, *Vol. 16, No. 5 (2018) 483-493*
DOI: https://doi.org/10.12989/gae.2018.16.5.483

Evolution of dynamic mechanical properties of heated granite subjected to rapid cooling

Tubing Yin*, Shuaishuai Zhang, Xibing Li and Lv Bai

School of Resources and Safety Engineering, Central South University, Changsha, Hunan, China

(Received March 29, 2018, Revised September 4, 2018, Accepted September 13, 2018)

Abstract. Experimental study of the deterioration of high-temperature rock subjected to rapid cooling is essential for thermal engineering applications. To evaluate the influence of thermal shock on heated granite with different temperatures, laboratory tests were conducted to record the changes in the physical properties of granite specimens and the dynamic mechanical characteristics of granite after rapid cooling were experimentally investigated by using a split Hopkinson pressure bar (SHPB). The results indicate that there are threshold temperatures (500-600ºC) for variations in density, porosity, and P-wave velocity of granite with increasing treatment temperature. The stress-strain curves of 500-1000ºC show the brittle-plastic transition of tested granite specimens. It was also found that in the temperature range of 200-400ºC, the through-cracks induced by rapid cooling have a decisive influence on the failure pattern of rock specimens under dynamic load. Moreover, the increase of crack density due to higher treatment temperature will result in the dilution of thermal shock effect for the rocks at temperatures above 500ºC. Eventually, a fitting formula was established to relate the dynamic peak strength of pretreated granite to the crack density, which is the exponential function.

Keywords: rapid cooling; thermal stress; physical properties; rock dynamic; crack density

1. Introduction

With the further growth of deep energy demand, the majority of engineering issues, such as the excavation of deep rock mass, development of geothermal energy, and so on, involve the mechanical properties of high-temperature rock. Some rock engineering, for example, enhanced geothermal systems, always suffers from rapid cooling, which results in a major physical deterioration process of the original rock. Consequently, studying the effects of sudden change in temperature on rocks has become a critical area of research in rock engineering.

Under high temperature, the anisotropy of mineral grains and the difference in the thermal expansion coefficient lead to thermal stress inside the rock, which can cause thermal cracking and can significantly change the physical properties of rock through the development of thermal cracks (Menendez *et al*. 1999). It should be noted that although many scholars have studied the effect of temperature on the physical and mechanical properties of rock through a variety of means (Chen *et al*. 2017, Jiao *et al*. 2015, Yin *et al*. 2015), many problems remain unsolved in applications where thermal stress is a vital factor. For example, in the drilling process of geothermal energy development, the use of drilling fluid will cool the high-temperature rock around the well, bringing about deterioration of the rock mechanical properties, which can promote rock failure during drilling (Zhang *et al*. 2013). However, it will cause deformation, cracks, and even collapse of boreholes as well, which will affect well completion. Moreover, deep underground excavations are subjected to cyclic thermal stresses due to rapid ventilation cooling and intermittent stoppages (Kim and Kemeny 2009). Historical monuments (Hajpál 2002), tunnels, and underground rock engineering may encounter a sharp drop of temperature owing to the use of physical methods to deal with fire accidents. As a consequence, the mechanical properties of rock change with the rock fracture penetration and thus lead to the structural failures.

In the above cases, the temperature of the rock has experienced a sudden drop. Meanwhile, the transient thermal stresses are generated during rapid cooling process, and stresses are normally tensile at the surface and compressive in the center of the body (Collin *et al*. 2002). The levels of transient thermal stresses are related to the rock initial temperature and temperature difference. The transient thermal stresses combined with the residual thermal stresses among mineral grains will cause cracks and further change material properties of high-temperature rock. Hence, considering the different temperatures, experimental characterizations of the rock response to rapid cooling are of great importance for various engineering applications.

To date, some scholars have investigated the petrophysical properties of heated rock after cooling (Somani *et al*. 2017, Tiskatine *et al*. 2016, Yin *et al*. 2016). Besides, Kumari *et al*. (2017) investigated the effect of cooling methods (both rapid and slow) on the mechanical behaviour of granite under uniaxial conditions. Shao *et al*. (2014) studied the influence of grain sizes on the response of heated granite specimens to cooling rate. Kim and Kemeny (2009) conducted laboratory tests to investigate the

*Corresponding author, Ph.D.
E-mail: tubing_yin@mail.csu.edu.cn

http://www.techno-press.org/?journal=gae&subpage=7
ISSN: 2005-307X (Print), 2092-6219 (Online)

effect of rapid cooling rock damage and found that because of the different lithology, crack growth occurred in some rock types, while crack healing occurred in others. Siratovich *et al*. (2015) carried out an investigation of the porosity, density, elastic moduli, and permeability of rocks subjected to rapid cooling using self-developed apparatus and reported that compared to slowly cooled samples, the rapidly cooled samples showed an increase in permeability. Xi *et al*. (2010) performed tests on the mechanical properties of granite treated by rapid cooling and showed that an abrupt change in the temperature of the rock mass cause the tensile strength of the granite to be negatively exponentially related to the temperature, with the elastic modulus and the temperature having a negative logarithmic function.

However, previous researches are limited to static test investigation of the variations in properties of the rock after rapid cooling. In engineering fields such as geological boring and mining in the deep recesses of the ground, the rock at depth is actually subjected to dynamic loading arising from blasting and boring (Li *et al*. 2008, Tao *et al*. 2016, Jeon *et al*. 2015). It is important to explore the impact of stress pulses or dynamic loads on rock failure (Tao *et al*. 2017), strength characteristics (Tao *et al*. 2017), and fracture propagation behaviour (Kim *et al*. 2018). In practice, considerably less attention has been paid to the dynamic mechanical properties of rock after rapid cooling. Until now, only Wang *et al*. (2016) reported that, under impact compression, the dynamical mechanical properties of red sandstone subjected to sudden changes in temperature were improved with the increase of strain rate. At a relative higher strain rate, the deterioration rates of both dynamic uniaxial compressive strength and deformation modulus were lower than those at a lower strain rate. Nevertheless, this study mainly focuses on the repeated rapid cooling response of rocks at a specific temperature (200ºC). For deep mining, enhanced geothermal systems (up to 350ºC (Sanchez-Alfaro *et al*. 2016)), and deep nuclear waste disposal facilities (up to 1000ºC (Gibb 2000)), a thorough understanding of the response of the rocks with different temperatures to rapid cooling treatment is necessary for engineering projects.

The purpose of this paper is to analyse the changes in physical properties and the damage to granite subjected to rapid cooling, with the temperature range of 25-1000ºC. Dynamic laboratory tests were also carried out for the measurement of the dynamic compressive properties of pre-treatment granite. Then, the work focuses on the evaluation of the rapid cooling effects on the dynamic characteristics of rocks by analysing the relationship between the crack density and the peak stress. The research results will provide a reliable basis for extraction of geothermal energy, deep rock mass construction, or potential nuclear waste disposal and will provide reasonable parameters for related numerical simulation tests.

2. Experimental study

2.1 Preparation and pretreatment of specimens

The fine-grained granite samples used in the test, which

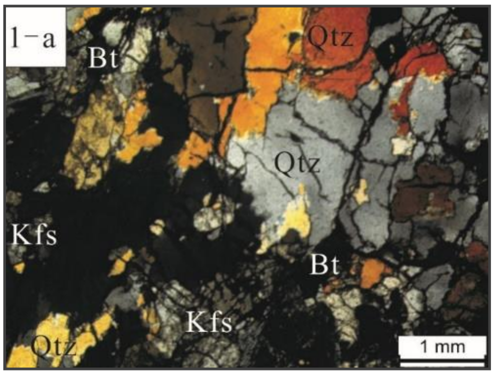

Fig. 1 Petrographic microscopy images of the granite

were mainly composed of quartz, feldspar, biotite, and a small amount of montmorillonite, were gathered from a quarry in Changsha, China. Three kinds of main mineral grains, that is, quartz, feldspar, and biotite, are marked in Fig. 1. According to the requirements of the International Society of Rock Mechanics (Zhou *et al*. 2011), cylindrical granite specimens 50 mm in diameter and 50 mm in length were polished to ensure that the two end planes of the sample were parallel with an accuracy of ± 0.05 mm and the surface roughness was within 0.02 mm for dynamic impact compression tests. These specimens were divided into eight groups for pretreatment.

Before pretreatment, the size, weight, and wave velocity of the samples were measured. Table 1 lists the fundamental parameters of the tested granite samples. Then the specimens were divided into 8 groups, and 7 of which were heated to the preset temperature, consisting of seven different temperature levels (100, 200, 400, 500, 600, 800, and 1000ºC), at a rate of 2ºC/min and maintained at the target temperature for 2 h. The heated rate can effectively avoid the temperature gradient-induced thermal shock during heating. After exposure to high temperatures, the samples were quickly removed from the oven and underwent rapid cooling in cold water. Because the heat transfer coefficient, which is defined as the thermal transmission in unit time to or from unit area of a surface in contact with its surroundings for unit difference between the temperature of the surface and the environmental fluid temperature (Dincer and Genceli 1994), for water cooling is in the range of 200-1400 W/m^2 K (Engineering ToolBox. 2013, Zhao 1987). And the value of free-convective heat transfer coefficient for air in natural cooling is within the typical range of 5-25 W/m^2 K (Park *et al*. 2014). Additionally, if the radiation heat transfer of rock sample is negligible and the heat transfer coefficient is assumed to be constant, the values of Biot number in two conditions of natural cooling and rapid cooling can be calculated by Eq. (1)

$$Bi = \frac{l_c h}{\lambda} \tag{1}$$

where l_c is characteristic length, which is commonly defined as the volume of the body divided by the surface area of the body; h is the heat transfer coefficient; λ is the thermal conductivity of the body.

Table 1 Values of fundamental parameters of granite

Parameter	Bulk density /(g/cm³)	V_p /(m/s)	V_s /(m/s)	Porosity /%	Compressive strength /MPa	Tensile strength /MPa
Value	2.776	4991.4	2824.8	0.286	172.86	9.71

Fig. 2 Flow diagram of experimental study

For high-temperature rock samples with same shapes, the value of Biot number for water-to-rock thermal conduction is at least ten times that of air-to-rock thermal conduction, which means that larger temperature gradient will be caused by the former. So the water cooling method was chosen to provide a corresponding cooling rate for high-temperature rock samples. And the water bath temperature of each specimen was 20°C.

When completely cooled to room temperature, the rock samples were put into a low-temperature drying box and dried to a constant weight. At the end of the pretreatment, measurements of the density loss and wave velocity loss were carried out again at room temperature. The process of experimental study is illustrated in Fig. 2.

2.2 Experimental setup

An AutoPore IV 9500 automatic mercury injection apparatus was used in the porosity test, as shown in Fig. 2. The working pressure range of the experimental system is 0-228 MPa and the range of diameters is 0.003-1000 μm. In the test, mercury was used as the non-infiltrating phase and invaded the pores of the samples under external pressure. The porosity can be calculated from the mercury content of the test samples. The mercury intrusion technique can also be used to calculate numerous sample properties such as pore size distributions and total pore volume. According to Washburn, the forced intrusion of liquid mercury between particles and into pores is a function of applied pressure. It can be expressed as

$$P = \frac{-4\tau\cos\theta}{D} \tag{2}$$

where P is capillary pressure; D stands for the pore diameter of the sample; τ represents the surface tension coefficient of mercury, taken as 0.48 N/m; and θ is the wetting angle of mercury with solid, taken as 140°. So the pore size distributions can be described by the corresponding capillary pressure.

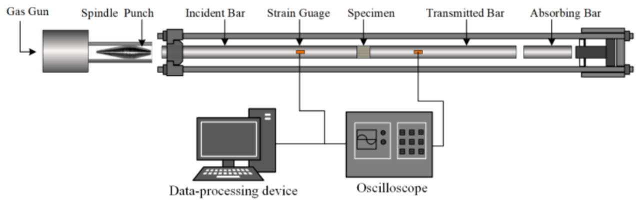

Fig. 3 Functional diagram of the Φ50 mm SHPB test system

In order to investigate the residual dynamic characteristics of heated granites subjected to rapid cooling, the impact loading test was carried out using a split Hopkinson pressure bar (SHPB) system that belongs to the School of Resources and Safety Engineering in Central South University. The test devices consist of a striker punch, an incident bar, a transmitted bar, an absorption bar, and a data acquisition unit. The spindle shaped punch and bars are made of high-strength nickel alloy steel with an ultimate strength of 800 MPa. The lengths of the incident bar, the transmitted bar, and the absorber bar are 2000, 1500, and 500 mm, respectively, and the diameters are 50 mm. The SHPB testing system is illustrated in Fig. 3. In the test, the high-speed spindle-shaped punch ejected by the gas gun can produce a half-sine wave and achieve a constant strain rate load on the specimen (Li *et al.* 2000). The dynamic strain gauge can record the voltage signals of the incident bar and the transmitted bar. Based on the recorded data, the stress, strain, and strain rate of the sample under impact compression can be calculated by Eq. (3)-(5) (Zhou *et al.* 2010)

$$\sigma(t) = \frac{A_e E_e}{2A_s}[\varepsilon_I(t) + \varepsilon_R(t) + \varepsilon_T(t)] \tag{3}$$

$$\varepsilon(t) = \frac{C_e}{L_s}\int_0^t [\varepsilon_I(t) - \varepsilon_R(t) - \varepsilon_T(t)]dt \tag{4}$$

$$\dot{\varepsilon}(t) = \frac{C_e}{L_s}[\varepsilon_I(t) - \varepsilon_R(t) - \varepsilon_T(t)] \tag{5}$$

where $\sigma(t)$, $\varepsilon(t)$, and $\dot{\varepsilon}(t)$ stand for the stress, strain, and strain rate functions of the specimen, respectively, and A_e, C_e, and E_e are the cross-sectional areas, wave velocity, and Young's modulus of the elastic bars. A_s and L_s are the cross-sectional area and length of the sample, while ε_I , ε_R, and ε_T, respectively, represent the incident, reflected, and transmitted strains of the bar.

3. Test results and analysis

3.1 Degradation of granite structure

After the pretreatment, that is, the rapid cooling test of heated granite with different temperatures, the impacts of the process on the high-temperature granite are obtained.

Fig. 4 Appearance of granite specimens after pretreatment

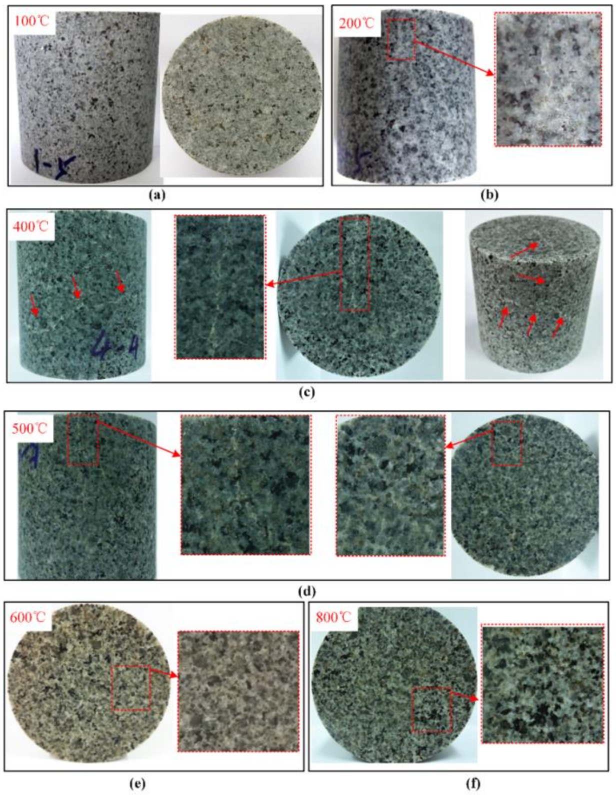

Fig. 5 The crack characteristics of granite after different pretreatment temperatures (The appearance of granite specimens is not accordant in Fig. 4 and Fig. 5, which is mainly due to differences in photography equipment and background)

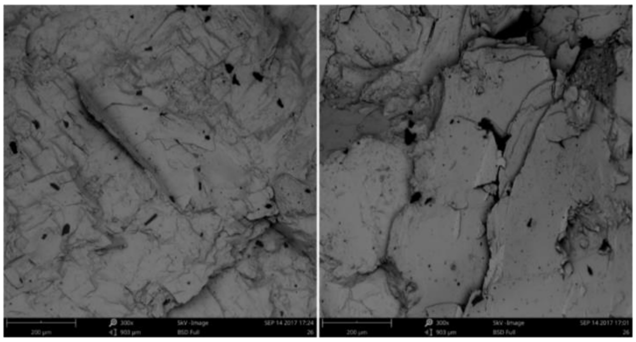

(a) T_p=20ºC

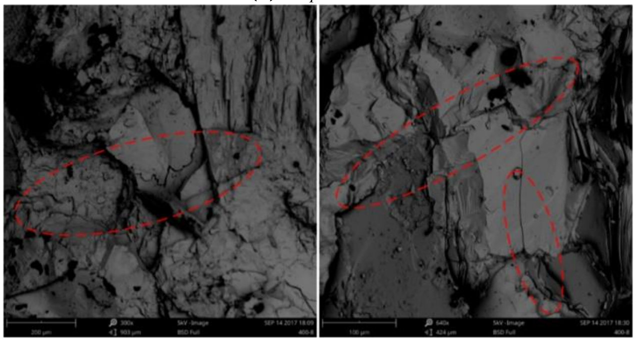

(b) T_p=400ºC

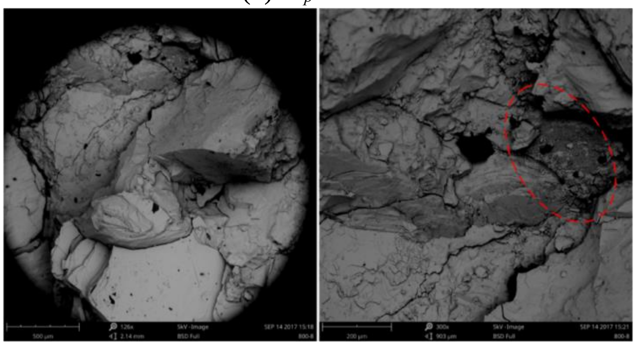

(c) T_p=800ºC

Fig. 6 SEM images of granite specimens with different temperatures after thermal shock: (a) Room temperature, (b) 400°C and (c) 800°C

Fig. 4 shows the appearance of the specimens. It is clear that the colour of the granite specimens becomes lighter (from dark grey to light brown) with increasing temperature and the colour of mineral grains visible to the naked eye, such as biotite, is more prominent, which are mainly caused by the mineral dehydration and the cement oxidation (Hajpál and Török 2004). The evolution of defects in the materials with increasing pretreatment temperature is reflected in Fig. 5; it can be seen that when the specimen is heated to 200ºC and subjected to rapid cooling, visible cracks appear on the sample surface. When the pretreatment temperature (T_p) is 400ºC, the sample surface shows obvious micro-cracks around the mineral grains. Through-cracks appear at the cylinder end and in the middle of the surface, as shown in Fig. 5(c). In most samples, the crack on the end surface extends to the middle transverse crack, which leads to the formation of a λ-shaped crack. When the pretreatment temperature is increased to 500ºC, the length and quantity of the through-cracks are significantly reduced compared with the samples that are heated to 400ºC. However, there are relatively short interpenetrating cracks extended along the quartz grains. When T_p > 500ºC, only randomly distributed intergranular micro-cracks can be observed.

Based on the experimental results, we consider that the thermal-gradient-induced stress can be the driving force of micro-crack propagation and the thermal gradient-induced cracks due to thermal shock and thermally induced cracks resulted from heating lead to degradation of granite structure. When the pretreatment temperature is relatively low, the temperature-gradient-induced stress results in the development of micro-cracks and the occurrence of macro-damage, and the thermal shock crack with preferred orientation eventually coalesces, as shown in Fig. 5(c). When the heating temperature exceeds 500ºC, with further increases in porosity, the existence of pores and micro-cracks can hinder the expansion and penetration of thermal gradient-induced cracks during rapid cooling, which indicates that the thermal shock effects are diluted.

The microstructures of the heated granite specimens subjected to thermal shock were identified by scanning electron microscopy (SEM). Three test samples were cut from the pretreatment granite specimens at temperatures of 20ºC, 400ºC and 800ºC, respectively. Fig. 6 shows the characteristic appearances of the sample surfaces with three different pretreatment temperatures. At room temperature, there is no obvious crack in Fig. 6(a). Meanwhile, the structure of the sample is complete and the surface is relatively smooth. It can be seen that there are micro-cracks emerging and the main cracking path exists transgranular cracks when the pretreatment temperature is 400ºC, while the mineral grains are still tightly bound, with no obvious boundary. When the granite specimen suffers from thermal shock at 800ºC, in contrast to initial rock, the crack density of the surface increases significantly and the SEM images show predominantly intergranular fracture. When the structure is magnified, the cement between the adjacent mineral grains loses cementation can be observed clearly, as shown in Fig. 6(c). Furthermore, increased crack density and dense distribution of intergranular cracks are in agreement with results reported in the mechanism analysis of crack pattern differences.

3.2 Effect of pretreatment on density of granite

The mean values and standard deviation of the density of the preprocessed granite are reported in Fig. 7. To avoid possible problems related to poor reproducibility of the measurements from sample to sample, the magnitude of the change before and after the pretreatment is also shown; it is defined as the ratio of the value of the pretreated specimen at a specific treatment temperature to the initial value of the specimen at room temperature. The overall trend of the change in density of the granite sample after pretreatment is an increase in the pretreatment temperature and a decrease of the granite density. When the pretreatment temperature rises from room temperature to 500ºC, granite shows weak sensitivity to temperature changes during rapid cooling, with a change of 0.75%. when the pretreatment temperature exceeds 600ºC, there is a sharp decrease in density. In particular, the sample density is reduced by 5.1% at the pretreatment temperature of 1000ºC.

Many laboratory studies have investigated the evolution of specimen density with various pretreatment methods and temperatures, as summarized in Table 2. The magnitude of the density variation is related to the type of rock, the temperature of the treatment, and the manner of cooling. The main reason for the change is the decrease of mass and the expansion of volume.

Our interpretation is as follows: (1) At temperatures from 100 to 500ºC, adhered water, bound water, and structural water of the specimen will escape at different temperatures, resulting in a decrease in the sample mass (Zhang *et al*. 2016). (2) At 575ºC, α/β phase transition of

Table 2 Summary of research on density change of heat-treated rock (Fan *et al*. 2017, Huang *et al*. 2017, Wang *et al*. 2017, Yang *et al*. 2017)

Rock type	Maximum temperature	Cooling-down method	Normalized value	Comments
Sandstone	800ºC	Natural cooling	0.965	Water escapes and the volume increases obviously from 400°C
Sandstone	200ºC	Rapid cooling (40 heating-cooling cycles)	0.969	Reduced by the adding up of heating-cooling cycles. Changes faster in the first few cycles
Granite	900ºC	Natural cooling	0.962	Expansion of mineral grains and crack formation
Granite	800ºC	Natural cooling	0.970	Can be neglected

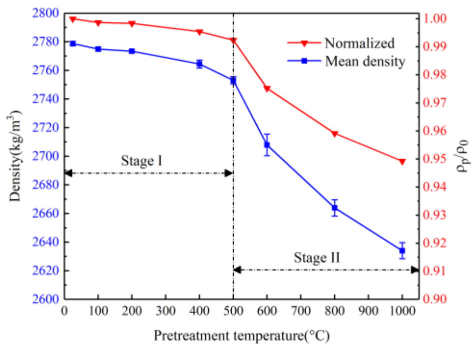

Fig. 7 Effect of pretreatment on the density

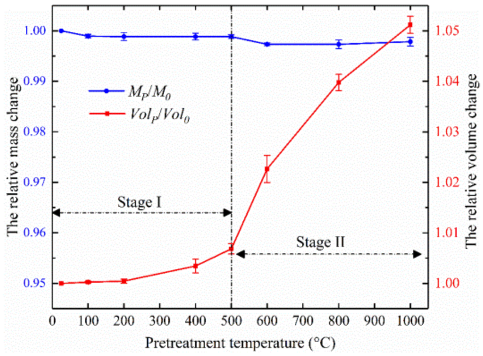

Fig. 8 The variation of mass and volume of granite specimens

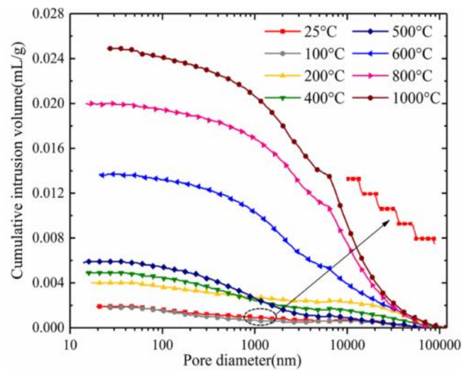

Fig. 9 Relationship between cumulative intrusion volume and pore diameter

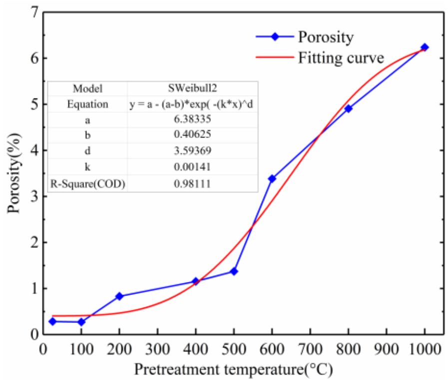

Fig. 10 Effect of pretreatment on the porosity

Table 3 Percentage of different pore sizes of granite at different pretreatment temperatures

Pretreatment temperature/ºC	Pore size distributions		
	10~100 μm/%	1~10 μm/%	<1 μm/%
25	36.84	10.53	52.63
100	31.58	5.26	63.16
200	57.50	10.00	32.50
400	30.61	18.37	51.02
500	15.26	28.81	55.93
600	28.47	46.71	24.82
800	37.00	47.00	16.00
1000	36.00	46.40	17.60

quartz will cause a volumetric increase (Glover *et al*. 1995). Then the micro-cracks induced by thermal fracture during heating (Takarli *et al*. 2008) and the rapid cooling process also contribute to volume expansion. Fig. 8 shows the relative changes in mass and volume of specimens with different pretreatment temperatures. With the increase of pretreatment temperature, there is a great change in volume compared with mass. And the rate of volume variation is obviously higher than that of the first stage, which is consistent with the variation of density. So the study indicated that the volume expansion caused by heat treatment is the main controlling factor for the decrease of sample density.

3.3 Effect of pretreatment on porosity of granite

Porosity is one of the most important physical characteristics governing the mechanical resistance and density of rocks (Tiskatine *et al*. 2016). Figs. 9 and 10 show the results of the mercury intrusion test, including the curve indicating the relation between pore size and mercury content and the curve of porosity variation. Fig. 9 shows that after low-temperature pretreatment of the sample, for example at 100ºC, the mercury injection curve has a stepped shape, indicating that the sample pore diameters are quite different. When the pretreatment temperature is higher, the mercury injection curve increases continuously, indicating the coexistence of multi-scale pores in the sample. Fig. 10 shows the influence of pretreatment on the porosity of granite. The total porosity ranges from 0.273 to 6.238%. The porosity of the original sample is 0.286%, whereas the porosity of the 100ºC sample is slightly lower than that of the original sample, dropping by 4.3%. which relates to the thermally induced volumetric expansion of the mineral grains. When the pretreatment temperature exceeds 100ºC, the porosity increases gradually with increases in pretreatment temperature. The fitting curve illustrated the connection between porosity Ψ and pretreatment temperature T_p can be expressed by fitting Eq. (6).

$$\Psi = a - (a - b) \times e^{-(kT_p)^d} \qquad (6)$$

The phase change and evaporation of water as well as the excessive concentration of thermal stress between the non-homogeneous mineral particles lead to intergranular cracks and connection of pores. It is worth noting that

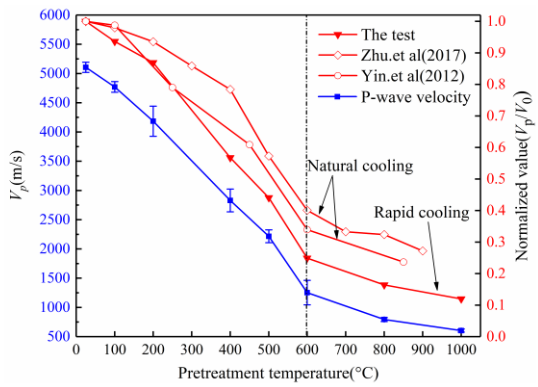

Fig. 11 Effect of pretreatment on the P-wave velocity

between 500 and 600ºC, the growth rate of porosity is relatively high, mainly induced by the phase transition of quartz.

According to the curve obtained by the mercury intrusion test, the pore size distributions of the heated samples subjected to rapid cooling can be obtained. The results are listed in Table 3. In normal condition, the 52.63% of pores in the original sample have diameters which are less than 1μm, belonging to the micro-pore. And only 10.53% of the pores belong to the medium pore. With the increase of pretreatment temperature, the percentage of micro-pore in the sample decreases gradually. When T_p=1000ºC, micro-pore accounts for 17.6%, while the proportion of medium pore with pore diameters from 1μm to 10μm expands to 46.4%, which indicates that the pretreatment makes most of the micro-pores develop, and transform into the medium pore. During the process, pores with pore size greater than 10 μm are not significantly affected.

3.4 Effect of pretreatment on P-wave velocity of granite

The P-wave attenuation can directly reflect the degree of damage within the rock. It is clear from Fig. 11 that the P-wave velocity of granite is strongly dependent on the pretreatment temperature. The average wave velocity of the intact granite samples is between 4950 and 5200 m/s. As the pretreatment temperature increases gradually, the P-wave velocity declines approximately linearly. The data show that when the pretreatment temperature is 600ºC, the mean value of the P-wave velocity decreases to 1250 m/s. The normalized value clearly shows that the P-wave velocity is reduced by 75% compared with the initial value. At 1000 ºC, the value decreases significantly by 88%. Some scholars have also studied the variation of P-wave velocity in order to evaluate granite that has been treated in different ways (Yin *et al*. 2012, Zhu *et al*. 2017). The trends of variation of the P-wave velocity are basically consistent with our test result.

However, the difference is that the change rate of the P-wave velocity induced by rapid cooling is obviously higher than that caused by natural cooling. To explain such a change of behaviour, the following arguments can be made: (1) The decrease in P-velocity with porosity is fairly linear (David *et al*. 1999) and the increased porosity induced by pretreatment causes a sharp decrease of P-wave velocity, according to data in Fig. 10. (2) The decrease of the P-wave velocity also results from cracks developed during the rapid cooling. When the T_p is higher than 200ºC, there are obvious through cracks and they gradually expand with the temperature increasing. In particular, transverse cracks have a strong resistance to the propagation of ultrasound. When the pretreatment temperature exceeds 600ºC, although the number of micro-cracks increases, the thermal shock effect is diluted, and the damage increment decreases. Accordingly, when the T_p > 600ºC, the rate of decline in the P-wave velocity gradually decreases. One of the reason is that there are fewer sources of weakness available to introduce further damage to the rock sample during heating (Yin *et al*. 2018). The other is the decrease of damage increment induced by thermal shock. In general, the rapid cooling process has a noticeable effect on the damage to high temperature granite, especially when the pretreatment temperature is below 600ºC, which was reflected in the rate of change in P-wave velocity.

3.5 Effect of pretreatment on the dynamic peak stress of granite

The self-developed *Φ*50 mm SHPB device was employed to investigate the dynamic characteristics of the granite specimens after thermal shock. According to the SHPB principles, dynamic stress equilibrium which is a prerequisite to any valid SHPB experiment should be satisfied. In this study, Fig. 12 shows the stress histories on both ends of the specimen in a typical test (specimen No. 1-3). It can be observed that the curve of the sum of the incident stress (In.) and reflected stress (Re.) almost overlaps with that of the transmitted stress (Tr.). Obviously, the condition of dynamic stress equilibrium on both sides of the rock sample is achieved.

In the experiment, one impact pressure of 0.9 MPa was applied to all the pretreatment samples to obtain the relationship of the pretreatment temperature and the dynamic mechanical properties of rock. The value of the incident energy, reflecting the incident wave intensity, was controlled in the range of 380-400 J. Typical axial dynamic stress-strain curves are plotted in Fig. 13. The stress-strain

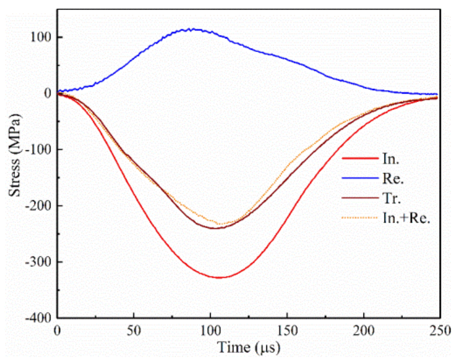

Fig. 12 Dynamic stress equilibrium check for a typical dynamic test

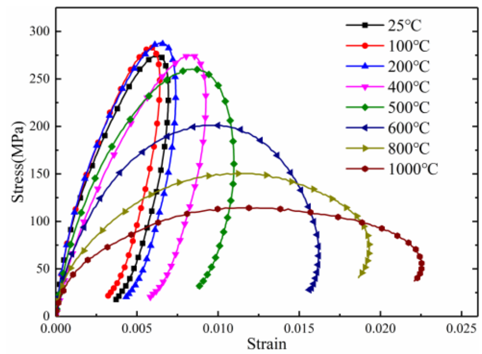

Fig. 13 Stress-strain curves of heated granite under impact loading after rapid cooling

Table 4 Results of dynamic compression test on pretreated granite rock

T_p/ºC	Sample no.	Incident energy/J	Peak stress /MPa	Peak strain	Elastic modulus /GPa
	0-1	384.46	255.96	0.00565	47.68
25	0-2	393.22	275.38	0.00622	47.16
	0-3	390.46	264.93	0.00617	46.99
	1-1	386.04	268.79	0.00647	46.94
100	1-3	380.10	252.11	0.00551	45.57
	1-4	391.27	282.95	0.00594	50.18
	2-1	392.08	237.96	0.00577	42.29
200	2-3	391.44	228.97	0.00506	43.61
	2-4	403.21	288.51	0.00647	51.09
	4-1	381.03	234.47	0.00603	37.92
400	4-3	385.32	274.62	0.00806	42.90
	4-4	402.83	246.29	0.00825	37.90
	5-2	390.89	225.68	0.00759	31.43
500	5-3	401.45	262.35	0.00799	42.82
	5-4	404.01	260.30	0.00880	41.50
	6-1	387.34	167.21	0.01045	20.41
600	6-2	386.71	167.01	0.01135	19.90
	6-3	403.84	201.04	0.01088	30.16
	8-1	387.37	150.35	0.01212	19.95
800	8-2	391.03	148.76	0.01150	18.30
	8-3	405.94	160.46	0.01213	20.69

Table 4 Continued

T_p/ºC	Sample no.	Incident energy/J	Peak stress /MPa	Peak strain	Elastic modulus /GPa
1000	10-1	396.42	114.61	0.01242	13.64
	10-2	396.40	114.24	0.01239	13.63
	10-3	393.78	119.92	0.01150	14.65

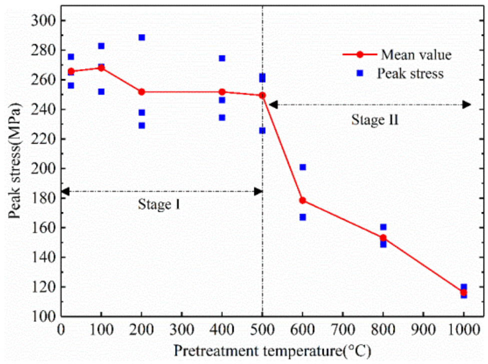

Fig. 14 Relationship between peak stress and pretreatment temperature

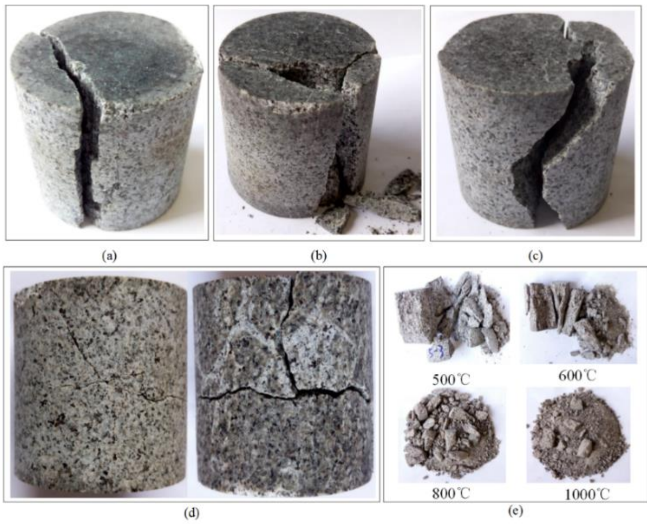

Fig. 15 The post-failure images of tested granite after different treatment temperatures: (a) T_p = 20ºC, (b) T_p = 100ºC, (c)T_p=200ºC, (d) T_p = 400ºC and (e) T_p=500~1000ºC

curve of the dynamic compression test consists of the elastic phase, the yield stage, and the failure stage. There is no significant difference in the stress-strain curves when the pretreatment temperature is 25-200ºC. The curve shows that when the limit of the elastic phase is reached, it immediately enters the failure stage, corresponding to the macro performance of the sample rupture. It should be noted that the rebound at the end of the curve is attributed to the incomplete broken of the specimen. When the pretreatment temperature is higher than 500ºC, the dynamic stress-strain curves show that the peak stress and the elastic modulus of the granite specimen decrease gradually as the processing temperature increases. The rapid cooling of specimens heated to 500ºC, 600°C, 800°C and 1000°C makes their elastic moduli reduces by around 18.4%, 50.3%, 58.5% and 70.5%. On the other hand, the yield platforms of curves, which represent the brittle-plastic transition between 500 and 1000ºC, are more obvious.

The mechanisms of the brittle-lastic transition during the pretreatment process can be summarized as follows. Firstly, the combined effect of irreversible thermally induced micro-cracks and the water escape causes an increase in the porosity of the rock specimen. Secondly, the rapid cooling effect leads to further development and coalescence of cracks in rock specimens. These changes contribute to the enhancement of dislocation defects. The macroscopic representation of the slip at the defect is plastic deformation during dynamic loading. Furthermore, the experimental results obtained according to the stress-strain curve are shown in Table 4.

It is clear from Fig. 14 that there is a downward trend of the peak stress in general with the increase in pretreatment temperature from 100 to 1000ºC. We noticed that the curve can be divided into two stages. At room temperature, the peak stress is 265.7 MPa. When the pretreatment temperature is below 500ºC, the rapid cooling process has little effect on the average peak stress of the specimen. In particular, the peak stress of the specimen under 100ºC treatment is slightly higher than that under room temperature treatment, which is resulted from the partial microcracks healing because of heating treatment. At the same time, the discrete values of the peak strength of specimens are larger, especially at 200 and 400ºC. The anisotropy of rocks contributes to the dispersion of peak strength. Besides, the dispersion of the peak strength is also influenced by the irregular cracks in the specimen which are caused by pretreatment. For instance, the effect of the cracks along the axial direction on the peak strength of the specimen is greater than that of the cracks perpendicular to the axial direction. After 500ºC, the average peak strength of the specimen is obviously reduced and the discreteness of the peak strength of each group decreases. Compared with the initial specimen, the average peak strengths of 600 and 1000ºC specimens decrease by around 32.8 and 56.3%, respectively.

3.6 Failure mode of pretreated granite

The representative failure patterns of dynamic loading tests at each temperature are given in Fig. 15. According to the results, the cracks developed during the process of rapid cooling have an appreciable impact on the rock failure mode. The dynamic compression failure mode of the original granite specimen is shown in Fig. 15(a). The specimen was divided into two parts by a clear split in the axial direction, which is the typical tensile failure for rocks. Since the tensile elongation at the same longitudinal plane of the specimen is substantially the same, the rupture plane is almost parallel to the axis. As shown in Fig. 15(b) and (c), after the processes of pretreatment, the samples treated at 100 and 200ºC were split into two halves along the loading axis, which is similar to the test sample at room temperature. However, due to the influence of cracks inside the specimens at 200ºC, the tensile strength of the weak surface is greatly reduced, so that the main rupture surface of the specimen is not completely parallel to the axial direction. It is interesting that the specimen whose pretreatment temperature was 400ºC was split into three parts along pre-existing cracks generated after pretreatment. Fig. 15(d) indicates that the λ-shaped crack caused by the rapid cooling plays a controlling role in the dynamic failure mode of the granite specimen. Fig. 15(e) shows that when the pretreatment temperature is higher than 500ºC, with increasing temperature, the degree of fragmentation of specimens decreases gradually. The specimen pretreated with 1000 ºC was struck into powder particles. Therefore, where the incident energy is the same, the higher the pretreatment temperature, the smaller the amount of energy required for rock breakage.

4. Discussion

The effect of rapid cooling on the structural change of high-temperature granite affects the failure model of the dynamic compression test. Meanwhile, the variation of the physical properties must affect the dynamic mechanical characteristics of specimens. Hence, the correlations between residual strength and the variation of physical properties after rapid cooling should be studied. The crack density *c*, which is defined as the ratio of the volume of the crack to the total rock volume (O'Connell *et al*. 1974), was introduced to characterize the cracks of pretreated specimens and to denote the degree of change in the physical properties.

According to our test, we theoretically assume that the rock specimen is isotropic material, which has been checked by measuring V_P in three perpendicular directions (the velocity variations are within 2% (Reuschlé *et al*. 2003)). Based on the Biot-consistent model (Thomsen 1985), the crack density of pretreated specimen *c* can be rearranged as follows (Byun *et al*. 2015)

$$c=\frac{\dfrac{\rho V_S{}^2}{G_S}+\dfrac{\psi}{1-\dfrac{2\times(4-5Y)}{15\times(1-Y)}}-1}{\dfrac{2\pi\alpha}{1-\dfrac{2\times(4-5Y)}{15\times(1-Y)}}-\dfrac{32\times(1-Y)(5-Y)}{45\times(2-Y)}} \tag{7}$$

where ρ denotes the unit weight of the specimen; G_s is the shear modulus of the particle; Ψ refers to the porosity; α represents the aspect ratio, which is the ratio of the shortest side to the longest side of the crack; and Y is defined as follows

$$Y=\frac{V_P^2-2V_S^2}{2(V_P^2-V_S^2)} \tag{8}$$

where V_P and V_S are the values of the P-wave and S-wave, respectively.

The equation indicates that the crack density, which is a function of the physical properties of the pretreated specimens, can be applied to investigate the connection of residual strength and physical properties.

Based on the results of Part 3, the calculated crack density is summarized in Table 5 (the S-wave velocity of the pretreated sample at 1000°C cannot be detected). The shear modulus of a grain and the aspect ratio are assumed to be 32.6 GPa and 0.001 (Tang 2011), respectively.

Table 5 Results of analysed crack density of pretreated specimens

Pretreatment temperature/ºC	P-wave velocity /(m/s)	S-wave velocity /(m/s)	Porosity /%	Crack density
25	5106.6	2890.0	0.286	0.1997
100	4771.2	2889.9	0.273	0.1904
200	4184.9	2544.9	0.832	0.2892
400	2830.1	1854.5	1.155	0.4262
500	2217.1	1460.1	1.373	0.4902
600	1253.9	830.8	3.385	0.5367
800	793.7	514.6	4.906	0.5526

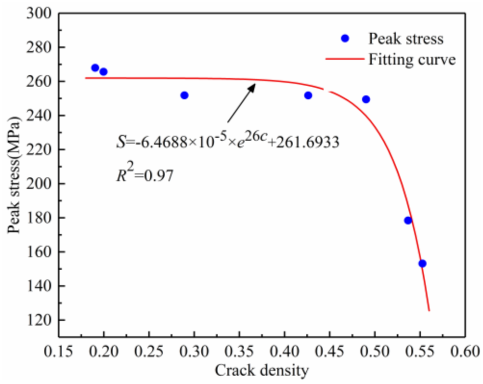

Fig. 16 Relationship between peak stress and crack density

Fig. 16 presents the relationship between crack density and peak stress at different pretreatment temperatures. To fully describe the dependence of the peak stress of granite after the rapid cooling on crack density, an experimental fitting formula under the pretreatment temperatures ranging from 25 to 800 ºC is proposed as follows

$$S=-6.4688\times10^{-5}\times e^{26c}+261.6933 \quad R^2=0.97 \tag{9}$$

where S is the predicted value of the dynamic peak stress and c is the crack density of granite subjected to rapid cooling.

The determination coefficient (R^2) proves that a good correlation has been established between dynamic peak stress and crack density. Meanwhile, the fitting curve reveals that the peak stress of the granite subjected to rapid cooling is sensitive to the crack density when the crack density is higher than 0.45.

5. Conclusions

The rock materials are heterogeneous materials consisting of different granular aggregates of polycrystalline mineral constituents from the perspective of their microstructure. During rapid cooling, without the presence of additional mechanical stresses, the degradation of the high-temperature rock mainly induced by cracking can be related to temperature gradient-induced stress and thermal stress between the grains. This is a qualitative understanding of the effect of thermal shock. Then, we evaluated the influence of rapid cooling on the physical properties, including the density, porosity, and wave velocity, as well as the dynamic mechanical property of granite rocks, by laboratory tests at various temperatures between 25 and 1000 ºC. The following conclusions can be drawn.

- The density and P-wave velocity exhibited reductions with increasing pretreatment temperature, and the porosity of pretreated granite specimens increased at the same time. Most importantly, the curves of variation of physical properties exhibit characteristic temperature points induced by the combined effect of water evaporation, thermally induced cracks, and crack connection.
- When the pretreatment temperature is 200-500ºC, the rapid cooling will cause the formation of macro-cracks in the granite specimens. Particularly at 400ºC, the dynamic tests showed that the λ-shaped induced crack has a decisive influence on the failure pattern of rock.
- The experimental fitting formula of the variation of physical properties and peak stress shows that the dynamic peak stress of granite subjected to rapid cooling decreases exponentially with increasing crack density.

Acknowledgements

The research presented in this paper was carried out under the joint financial support of the National Natural Science Foundation of China (No. 51774325), the Hunan Provincial Natural Science Foundation of China (No. 2017JJ3389), the Innovation-Driven Project of Central South University (No. 2017CX006), the State Key Research Development Program of China (No. 2016YFC0600706), and the State Key Program of National Natural Science Foundation of China (No. 41630642). Technical support from the National Engineering Laboratory for High Speed Railway Construction for the porosity test is also appreciated.

References

Byun, J.H., Lee, J.S., Park, K. and Yoon, H.K. (2015), "Prediction of crack density in porous-cracked rocks from elastic wave velocities", *J. Appl. Geophys*., **115**, 110-119.

Chen, G.Q, Li, T.B, Wang, W. Guo, F. and Yin, H.Y. (2017), "Characterization of the brittleness of hard rock at different temperatures using uniaxial compression tests", *Geomech. Eng*., **13**(1), 63-77.

Collin, M. and Rowcliffe, D. (2002), "The morphology of thermal cracks in brittle materials", *J. Eur. Ceram. Soc*. **22**(4), 435-445.

David, C., Menéndez, B. and Darot, M. (1999), "Influence of stress-induced and thermal cracking on physical properties and microstructure of La Peyratte granite", *Int. J. Rock Mech. Min. Sci*., **36**(4), 433-448.

Dincer, I. and Genceli, O.F. (1994), "Cooling process and heat transfer parameters of cylindrical products cooled both in water and in air", *Int. J. Heat Mass Trans*., **37**(4), 625-633.

Engineering ToolBox (2013), Heat Transfer Coefficient, <http://www.engineeringtoolbox.com>.

Fan, L.F, Wu, Z.J, Wan, Z. and Gao, J.W. (2017), "Experimental investigation of thermal effects on dynamic behavior of granite", *Appl. Therm. Eng*., **125**, 94-103.

Gibb, F.G.F. (2000), "A new scheme for the very deep geological disposal of high-level radioactive waste", *J. Geol. Soc*., **157**(1), 27-36.

Glover, P., Baud, P., Darot, M., Meredith, P., Boon, S., LeRavalec, M., Zoussi, S. and Reuschle, T. (1995), "α/β phase transition in quartz monitored using acoustic emissions", *Geophys. J. Int*., **120**(3), 775-782.

Hajpál, M. (2002), "Changes in sandstones of historical monuments exposed to fire or high temperature", *Fire Technol*., **38**(4), 373-382.

Hajpál, M. and Török, A. (2004), "Mineralogical and colour changes of quartz sandstones by heat", *Environ. Geol*., **46**(3-4), 311-322.

Hall, K. (1999), "The role of thermal stress fatigue in the breakdown of rock in cold regions", *Geomorphology*, **31**(1-4), 47-63.

Huang, Y.H., Yang, S.Q., Tian, W.L., Zhao, J., Ma, D. and Zhang, C.S. (2017), "Physical and mechanical behavior of granite containing pre-existing holes after high temperature treatment", *Arch. Civ. Mech. Eng*., **17**(4), 912-925.

Jahan Bakhsh, K., Nakagawa, M., Arshad, M. and Dunnington, L. (2017), "On heat and mass transfer within thermally shocked region of enhanced geothermal system", *Geofluids*.

Jeon, S., Kim, T.H. and You, K.H. (2015), "Characteristics of crater formation due to explosives blasting in rock mass", *Geomech. Eng*., **9**(3), 329-344.

Jiao, Y.Y., Zhang, X.L., Zhang, H.Q., Li, H.B., Yang, S.Q. and Li, J.C. (2015), "A coupled thermo-mechanical discontinuum model for simulating rock cracking induced by temperature stresses", *Comput. Geotech*., **67**, 142-149.

Kim, E., Garcia, A. and Changani, H. (2018), "Fragmentation and energy absorption characteristics of Red, Berea and Buff sandstones based on different loading rates and water contents", *Geomech. Eng*., **14**(2), 151-159.

Kim, K. and Kemeny, J. (2009), "Effect of thermal shock and rapid unloading on mechanical rock properties", *Proceedings of the 43rd US Rock Mechanics Symposium and 4th US-Canada Rock Mechanics Symposium*, Asheville, North Carolina, U.S.A., June.

Kumari, W.G.P, Ranjith, P.G, Perera, M.S.A, Chen, B.K. and Abdulagatov, I.M. (2017), "Temperature-dependent mechanical behaviour of Australian Strathbogie granite with different cooling treatments", *Eng. Geol*., **229**, 31-44.

Li, X.B., Lok, T.S., Zhao, J. and Zhao, P.J. (2000), "Oscillation elimination in the Hopkinson bar apparatus and resultant complete dynamic stress-strain curves for rocks", *Int. J. Rock Mech. Min. Sci*., **37**(7), 1055-1060.

Li, X.B., Zhou, Z.L., Lok, T.S., Hong, L. and Yin, T.B. (2008), "Innovative testing technique of rock subjected to coupled static and dynamic loads", *Int. J. Rock Mech. Min. Sci*., **45**(5), 739-748.

Menendez, B., David, C. and Darot, M. (1999), "A study of the crack network in thermally and mechanically cracked granite samples using confocal scanning laser microscopy", *Phys. Chem. Earth Part A Solid Earth Geodesy*., **24**(7), 627-632.

O'Connell, R.J. and Budiansky, B. (1974), "Seismic velocities in dry and saturated cracked solids", *J. Geophys. Res*., **79**(35), 5412-5426.

Park, D., Park, E.S. and Sunwoo, C. (2014), "Heat transfer and mechanical stability analyses to determine the aspect ratio of rock caverns for thermal energy storage", *Solar Energy*, **107**(5), 171-181.

Reuschlé, T., Haore, S.G. and Darot, M. (2003), "Microstructural control on the elastic properties of thermally cracked granite", *Tectonophysics*, **370**(1-4), 95-104.

Sanchez-Alfaro, P., Reich, M., Arancibia, G., Pérez-Flores, P., Cembrano, J., Driesner, T., Lizama, M., Rowland, J., Morata, D., Heinrich, C.A., Tardani, D. and Campos, E. (2016), "Physical, chemical and mineralogical evolution of the Tolhuaca geothermal system, southern Andes, Chile: Insights into the interplay between hydrothermal alteration and brittle deformation", *J. Volcanol. Geotherm. Res.*, **324**, 88-104.

Shao, S.S., Wasantha, P.L.P., Ranjith, P.G. and Chen, B.K. (2014), "Effect of cooling rate on the mechanical behavior of heated Strathbogie granite with different grain sizes", *Int. J. Rock Mech. Min. Sci.*, **70**, 381-387.

Siratovich, P.A., Villeneuve, M.C., Cole, J.W., Kennedy, B.M. and Bégué, F. (2015), "Saturated heating and quenching of three crustal rocks and implications for thermal stimulation of permeability in geothermal reservoirs", *Int. J. Rock Mech. Min. Sci.*, **80**, 265-280.

Somani, A., Nandi, T.K., Pal, S.K. and Majumder, A.K. (2017), "Pre-treatment of rocks prior to comminution-A critical review of present practices", *Int. J. Min. Sci. Technol.*, **27**(2), 339-348.

Takarli, M. and Prince-Agbodjan, W. (2008), "Temperature effects on physical properties and mechanical behavior of granite: Experimental investigation of material damage", *J. ASTM Int.*, **5**(3), 1-13.

Tang, S.B., Zhang, H., Tang, C.A. and Liu, H.Y. (2016), "Numerical model for the cracking behavior of heterogeneous brittle solids subjected to thermal shock", *Int. J. Solid. Struct.*, **80**, 520-531.

Tang, X.M. (2011), "A unified theory for elastic wave propagation through porous media containing cracks-An extension of Biot's poroelastic wave theory", *Sci. China Earth Sci.*, **54**(9), 1441.

Tao, M., Chen, Z.H., Li, X.B., Zhao, H.T. and Yin, T.B. (2016), "Theoretical and numerical analysis of the influence of initial stress gradient on wave propagations", *Geomech. Eng.*, **10**(3), 285-296.

Tao, M., Ma, A., Cao W.Z., Li, X.B. and Gong, F.Q. (2017), "Dynamic response of pre-stressed rock with a circular cavity subject to transient loading", *Int. J. Rock Mech. Min. Sci.*, **99**, 1-8.

Tao, M., Zhao, H.T. and Li X.B. (2017). "Determination of spalling strength of rock by incident waveform", *Geomech. Eng.*, **12**(1), 1-8.

Thomsen, L. (1985), "Biot-consistent elastic moduli of porous rocks: Low-frequency limit", *Geophysics*, **50**(12), 2797-2807.

Tiskatine, R., Eddemani, A., Gourdo, L., Abnay, B., Ihlal, A., Aharoune, A. and Bouirden, L. (2016), "Experimental evaluation of thermo-mechanical performances of candidate rocks for use in high temperature thermal storage", *Appl. Energy*, **171**, 243-255.

Wang, P., Xu, J.Y., Fang, X.Y., Wen, M., Zheng, G.H. and Wang, P.X. (2017), "Dynamic splitting tensile behaviors of red-sandstone subjected to repeated thermal shocks: Deterioration and micro-mechanism", *Eng. Geol.*, **223**, 1-10.

Wang, P., Xu, J.Y., Liu, S.H. and Wang, H.Y. (2016), "Dynamic mechanical properties and deterioration of red-sandstone subjected to repeated thermal shocks", *Eng. Geol.*, **212**, 44-52.

Xi, B.P. and Zhao, Y. (2010), "Experimental research on mechanical properties of water-cooled granite under high temperatures within 600◦C", *Chin. J. Rock Mech. Eng.*, **29**(5), 892-897.

Yang, S.Q., Xu, P., Li, Y.B. and Huang, Y.H. (2017), "Experimental investigation on triaxial mechanical and permeability behavior of sandstone after exposure to different high temperature treatments", *Geothermics*, **69**, 93-109.

Yin, T.B., Bai, L., Li, X., Li, X.B. and Zhang, S.S. (2018), "Effect of thermal treatment on the mode I fracture toughness of granite under dynamic and static coupling load", *Eng. Fract. Mech.*, **199**, 143-158.

Yin, T.B., Li, X.B., Cao, W.Z. and Xia, K.W. (2015), "Effects of thermal treatment on tensile strength of Laurentian granite using Brazilian test", *Rock Mech. Rock Eng.*, **48**(6), 2213-2223.

Yin, T.B., Li, X.B., Xia, K.W. and Huang, S. (2012), "Effect of thermal treatment on the dynamic fracture toughness of Laurentian granite", *Rock Mech. Rock Eng.*, **45**(6), 1087-1094.

Yin, T.B., Wang, P., Li, X.B., Wu, B.B., Tao, M. and Shu, R.H. (2016), "Determination of dynamic flexural tensile strength of thermally treated laurentian granite using semi-circular specimens", *Rock Mech. Rock Eng.*, **49**(10), 3887-3898.

Zhang, H.Y., Gao, D.L., Salehi, S. and Guo, B.Y. (2013), "Effect of fluid temperature on rock failure in borehole drilling", *J. Eng. Mech.*, **140**(1), 82-90.

Zhang, W.Q., Sun, Q., Hao, S.Q., Geng, J.S. and Lv, C. (2016), "Experimental study on the variation of physical and mechanical properties of rock after high temperature treatment", *Appl. Therm. Eng.*, **98**, 1297-1304.

Zhao, J. (1987), "Experimental studies of the hydro-thermo-mechanical behavior of joints in granite", Ph.D Dissertation, Imperial College, London, U.K.

Zhou, Y.X., Xia, K.W., Li, X.B., Li, H.B., Ma, G.W., Zhao, J., Zhou, Z.L. and Dai, F. (2011), *Suggested Methods for Determining the Dynamic Strength Parameters and Mode-I Fracture Toughness of Rock Materials*, in *The ISRM Suggested Methods for Rock Characterization, Testing and Monitoring: 2007-2014*, Springer, Cham, Switzerland.

Zhou, Z.L., Li, X.B., Ye, Z.Y. and Liu, K.W. (2010), "Obtaining constitutive relationship for rate-dependent rock in SHPB tests", *Rock Mech. Rock Eng.*, **43**(6), 697-706.

Zhu, S.Y., Zhang, W.Q., Sun, Q., Deng, S., Geng, J.S. and Li, C.M. (2017), "Thermally induced variation of primary wave velocity in granite from Yantai: Experimental and modeling results", *Int. J. Therm. Sci.*, **114**, 320-326.

CC